Queuing Network Modeling of a Real-Time Psychophysiological Index of Mental Workload—P300 in Event-Related Potential (ERP)

Changxu Wu, Yili Liu, *Member, IEEE*, and Christine M. Quinn-Walsh

***Abstract*—Modeling and predicting of mental workload are among the most important issues in studying human performance in complex systems. Ample research has shown that the amplitude of the P300 component of event-related potential (ERP) is an effective real-time index of mental workload, yet no computational model exists that is able to account for the change of P300 amplitude in dual-task conditions compared with that in single-task situations. We describe the successful extension and application of a new computational modeling approach in modeling P300 and mental workload—a queuing network approach based on the queuing network theory of human performance and neuroscience discoveries. Based on the neurophysiological mechanisms underlying the generation of P300, the current modeling approach accurately accounts for P300 amplitude both in temporal and intensity dimensions. This approach not only has a basis in its biological plausibility but also has the ability to model and predict workload in real time and can be applied to other applied domains. Further model developments in simulating other dimensions of mental workload and its potential applications in adaptive system design are discussed.**

***Index Terms*—Computational modeling, dual task, event-related potential (ERP), mental workload, P300, queuing network.**

I. Introduction

MENTAL workload is one of the most important issues in studying human performance in complex systems [3]–[5]. Overloaded operators are more likely to make errors, reducing the safety of human–machine systems [4]. From the system engineering perspective, modeling and predicting mental workload at an early stage in system design are very helpful to reduce the mental workload of operators [4], [3]. Moreover, designing adaptive user interface in "real-time human engineering" expects real-time prediction of mental workload, so that the user interface can propose corresponding actions to keep operator mental workload at an optimal value [72]. In addition, there is a growing research field in human factors called neuroergonomics, which focuses on the investigation of the neural bases of mental functions and physical performance in applied domains [71]. If a computational model can bridge the neural activities (measured by event-related potential (ERP) or functional magnetic resonance imaging technique) and mental workload, it might be a useful tool to assist researchers in human factors to understand the basic mechanisms of mental workload and design the interface to optimize the workload.

To measure changes in mental workload in real time, event-related brain potential measurements stand out to be one of the most effective indexes of mental workload in comparison with some other behavioral, subjective, and psychophysiological measurements [7]. There are several advantages in using the ERP technique to measure mental workload. First, it provides a relatively continuous record of data over time, meeting the requirement of real-time human engineering. Second, it is not obtrusive to task performance because it does not require overt responses which are needed in measuring mental workload with secondary-task measurements. Third, compared with some other physiological measurements such as the pupil diameter which is sensitive to all information stages including perceptual, cognitive, and motor processing, ERP (e.g., P300 component) is diagnostic and sensitive to stimulus evaluation process (perceptual and central processing resources) but not motor execution process [7].

Ample ERP research has shown that the amplitude of the P300 component in the ERP typically reflects the current state of mental workload [9]–[13], [87]. P300 is a positive component characterized by a parietally maximal scalp distribution and a latency between 300 and 800 ms [13]. Here, latency refers to the time interval between the arrival of stimulus and the time point when the peak of the potential is observed. Because of its ease in measurement, P300 has become the most frequently measured ERP component. The most important finding of P300 related to mental workload is that the P300 amplitude (peak value) of a secondary task is reduced in dual-task conditions compared with that in the corresponding single-task situation of performing the secondary task alone, and the P300 amplitude of the secondary task decreases further when the difficulty of the primary task increases [5], [14], [15]. The study of Wickens *et al.* [14] is a representative study among the studies on this topic and is therefore selected as the target experiment for modeling in this paper (a detailed description of their experiment is in the modeling section of this paper).

To model P300 in accordance with its biological realism—an important requirement for building cognitive models [16], it

Manuscript received March 14, 2006; revised February 18, 2007, July 26, 2007, and November 15, 2007. This paper is based on work supported by the National Science Foundation under Grant NSF 0308000. This paper was recommended by Associate Editor Y. Xiao.

C. Wu was with the Department of Industrial and Operations Engineering, University of Michigan, Ann Arbor, MI 48109 USA. He is now with the Department of Industrial and Systems Engineering, State University of New York, Buffalo, NY 14260-2050 USA (e-mail: changxu@buffalo.edu).

Y. Liu is with the Department of Industrial and Operations Engineering, University of Michigan, Ann Arbor, MI 48109 USA.

C. M. Quinn-Walsh is with the Department of Anesthesiology, University of Michigan, Ann Arbor, MI 48109 USA.

Color versions of one or more of the figures in this paper are available online at http://ieeexplore.ieee.org.

Digital Object Identifier 10.1109/TSMCA.2008.2001070

is desirable to introduce the physiological mechanism underlying the generation of P300 discovered in neuroscience studies. Several researchers have proposed that P300 results from intracortical currents which are triggered by the release of norepinephrine (NE) [17], [18]. NE, originally described as a "classical neurotransmitter" (presumably because of its early discovery and its effects in peripheral systems) [70], is now viewed as a neuromodulator because of its role in central neural system: rather than producing direct excitatory or inhibitory effects on postsynaptic neurons, NE modulates such effects produced by other neurotransmitters such as glutamate and gamma aminobutyric acid [70]; NE also alters the "signal-to-noise ratio" of response evoked by other afferents, both excitatory and inhibitory, enhancing synaptic transmission in target circuits. Such modulatory effects have since been described for NE in many brain circuits in synaptic transmission and have been shown to be mediated, via different transduction mechanisms, by both β and α_1-adrenergic receptors [88]–[93].

NE is produced by the locus coeruleus–NE (LC–NE) system (a nucleus in the pontine regions of the brain stem that consists of NE-containing cells) [17], [21]; the LC–NE system synthesizes the NE and then sends it to the central nervous system via its efferent projections. NE is released in certain brain regions (known as P300 generators), causing a change of conductivity of these regions and then producing a change of the amplitude of P300 [17]. Nieuwenhis *et al.* [17] reviewed the major findings on the generators of P300 and found that P300 generators are mainly located in the prefrontal cortex, the medial temporal lobe structures (including the hippocampus), the temporal–parietal junction, and adjacent areas which are responsible for perceptual processing.

Aside from the experimental studies of the P300 component related to mental workload and its mechanism, it is necessary to review the related computational models of mental workload, ERP, and the LC–NE system.

In human factors engineering, several models of mental workload have been successfully developed, and they can be categorized into the following three groups: conceptual models, mathematical and simulation models, and task-analytic models. Among the conceptual models, Wickens' resource model [22] is one of the most influential models, and it describes how the amplitude and latency of the P300 component is related to the "resource" in cognitive information processing. In his model, the amplitude of the P300 component of the secondary task reflects the perceptual–cognitive resources which are depleted by the primary task [22]. Among the mathematical and simulation models, the representative models include control-theory-based model [23], queuing-theory-based model [24], [25], procedure-oriented crew model [26], Micro-SAINT [27], human operator simulator [28], mathematical model [29], and model human processor (MHP) [30]. Unlike the models of ERP and the LC–NE system which focus on the biological aspect of the cognitive system, these models emphasize their engineering applications, and the definition of mental workload varies based on the feature of the model itself. For example, Rouse's queuing theory model [25] regards the server utilization as a representation of mental workload. The task-analytic models include time line analysis and prediction model [31], task analysis/workload [32], workload index [33], and Bi and Salvendy's model [34] (see [3]–[6] for a comprehensive review of these models).

Different from the models in human factors engineering, the models introduced in the following section focus on the physiological and biological mechanisms in generating ERP waves. In modeling ERP and electroencephalography (EEG), several mathematical and simulation models have been successfully established [35]–[38]. Building on a lumped-parameter model, Jansen and Rit [37] developed a computational model to produce EEG rhythms. Based on Jansen and Rit's model, a neural mass model proposed by David and Friston [36] assumed that the behavior of a population of neurons (millions of interacting neurons) can be approximated using several state variables (e.g., mean membrane currents, potentials, and firing rates). The model reproduced brain signals within the oscillatory regime by simply changing the population kinetics.

In modeling the LC–NE system, several neural network models have been developed successfully [18], [39]. These models usually include several layers of connectionist units representing detection/input, decision, and response. These layers are connected with excitatory and inhibitory connections, and the weights of these connections are updated during the learning process. The model of Nieuwenhuis *et al.* [18] is able to successfully simulate LC activity and output of NE from the LC–NE system. Based on the LC activity and NE output, their model quantifies the attentional blink—a temporary deficit in processing of a target stimulus following successful processing of a previous target.

In sum, each of these models demonstrates its usefulness and ability to quantify one or several aspects of mental workload, ERP, or the LC–NE system. However, none of these models quantifies the major finding of P300 amplitude and latency related to mental workload based on its physiological mechanisms. As suggested by Olsen and Olsen [40], modeling mental workload remains to be a challenge in cognitive modeling, even though overt behavior (reaction time and response accuracy) has been modeled by existing models more successfully.

In this paper, we describe a queuing network modeling approach to quantify human performance and P300 as one of the most important psychophysiological indexes of mental workload, focusing on both biological realism of mental workload and its engineering application. First, we introduce the platform of this modeling approach—a simulation model of a queuing network architecture representing information processing in the brain. Second, based on this network platform, a set of mathematical equations is developed and implemented into the simulation model to quantify the amplitude and latency of P300. Third, the modeling results are presented and validated with the results of the representative experimental study of Wickens *et al.* [14]. Finally, we discuss the implication of the modeling approach and its further extensions to model the experimental results of other electrophysiological and human factors studies.

II. Queuing Network Modeling of Human Performance

In modeling human performance, computational models based on queuing networks have successfully integrated a large number of mathematical models in response time [1] and in multitask performance [2] as special cases of queuing networks. Moreover, it unifies the two isolated major groups in reaction

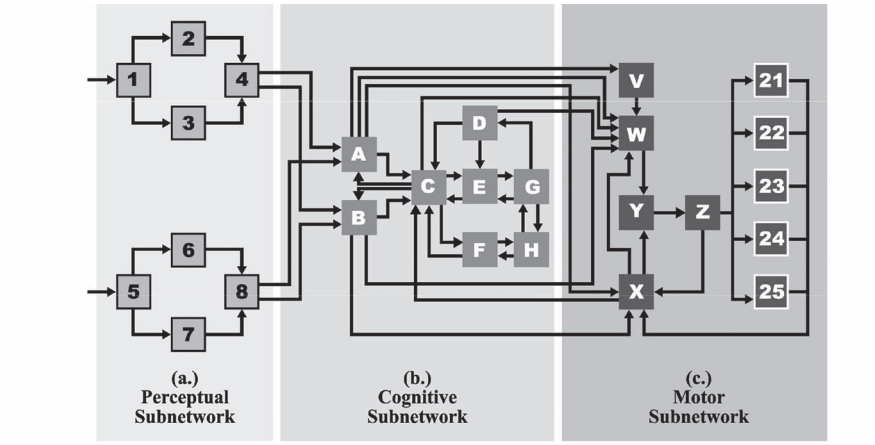

Perceptual Subnetwork	Cognitive Subnetwork	Motor Subnetwork
1. Common visual processing	A. Visuospatial sketchpad	V. Sensorimotor integration
2. Visual recognition	B. Phonological loop	W. Motor program retrieval
3. Visual location	C. Central executive	X. Feedback information collection
4. Visual recognition and location integration	D. Long-term procedural memory	Y. Motor program assembling and error detecting
5. Common auditory processing	E. Performance monitor	Z. Sending information to body parts
6. Auditory recognition	F. Complex cognitive function	21-25: Body parts: eye, mouth, left hand, right hand, foot
7. Auditory location	G. Goal initiation	
8. Auditory recognition and location integration	H. Long-term declarative & spatial memory	

(a)

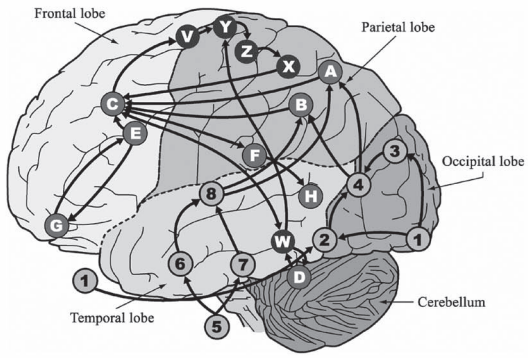

(b)

Fig. 1. (a) General structure of the queuing network model [55], [62], [84], [95], [96] and (b) the approximate mapping of servers in the queuing network model onto the human brain [55], [84], [95], [96].

time models (e.g., cascade model and program evaluation and review technique networks) and response accuracy models (e.g., accumulator and diffusion models) [41]. A simulation model of a queuing network mental architecture, called the queuing network–MHP (QN–MHP), has been developed to represent information processing in the mental system as a queuing network on the basis of neuroscience and psychological findings. Ample research evidence has shown that major brain areas with certain information processing functions are localized and connected with each other via neural pathways [20], [42]–[44], which is highly similar to a queuing network of servers that can process entities traveling through the routes serially or/and in parallel, depending on specific network arrangements. Therefore, brain regions with similar functions can be regarded as servers, and neural pathways connecting them are treated as routes in the queuing network (see Figs. 1 and 2). Furthermore, it has been discovered that information processed in the brain is coded in population spike trains [45]; depending on different tasks and learning stages, the to-be-processed information represented by these spike trains is sometimes processed by the brain regions (servers) immediately. Sometimes, they have to be maintained in certain regions to wait for the previous spike trains finishing their processing [46]. Hence, these spike trains can be regarded as one type of entity in the queuing network. Population spike trains transmitting through different brain regions require various neuromodulators to initiate and maintain behavioral and forebrain neuronal activity, which are essential for the collection and processing of sensory information [21]; these neuromodulators are regarded as the second type of entities in the queuing network.

QN–MHP is a task-independent cognitive architecture and has been successfully used to generate human behavior in real time, including simple and choice reaction time [47], transcription typing [58], [96], psychological refractory period [59], visual search [60], and driver performance [61]. Moreover, QN–MHP is able to account for the subjective mental workload measured by NASA-task load index [94] and brain imaging data in the transcription typing task [62].

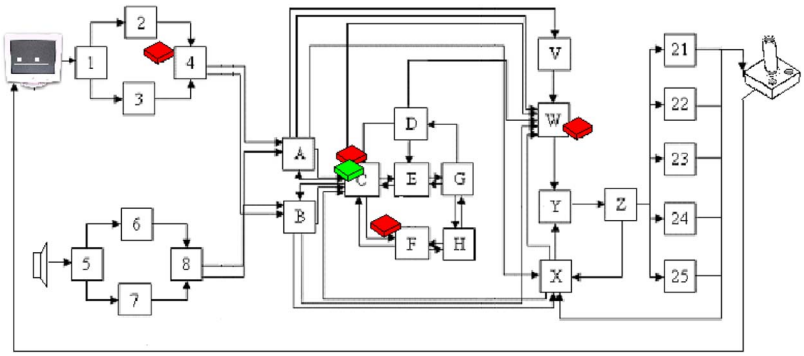

Fig. 2. Components of the simulation model (QN–MHP) in simulating the concurrent task: (Red entities) The manual tracking task and (green entities) the audio probe counting task.

The QN–MHP consists of the following three subnetworks: perceptual, cognitive, and motor subnetworks as described in the following sections.

A. Perceptual Subnetwork

The perceptual subnetwork includes a visual and an auditory perceptual subnetwork, with each of which being composed of four servers. In the visual perceptual subnetwork, light waves (represented by numerical codes) are transmitted to neuron signal (represented by information entities) at the eye, the lateral geniculate nucleus, the superior colliculus, the primary visual cortex, and the secondary visual cortex (represented by Server 1) [20]. Then, these entities are transmitted in parallel visual pathways—the parvocellular stream (represented by Server 2) and the magnocellular stream (Server 3) where the object content features (e.g., color, shape, labeling, etc.) and location features (e.g., spatial coordinates, speed, etc.) are processed [44], [48]. The distributed parallel area (represented by Server 4)—including the neuron connections between V3 and V4 as well as V4 and V5, the superior frontal sulcus, and the inferior frontal gyrus—integrates the information of these features from the two visual pathways and generates integrated perception of the objects [20], [47].

The auditory perceptual subnetwork also contains the following four servers: the middle and the inner ear (represented by Server 5[1]) transmits sound to parallel auditory pathways, including the neuron pathway from the ventral cochlear nucleus to the superior olivary complex (represented by Server 7) and the neuron pathway from the dorsal and ventral cochlear nuclei to the inferior colliculus (Server 6) where location, pattern, and other aspects of the sound are processed [20]. The auditory information in the auditory pathways is integrated at the primary auditory cortex and the planum temporale (represented by Server 8) [49].

B. Cognitive Subnetwork

The cognitive subnetwork includes a working memory system, a goal execution system, a long-term memory system, and a complex cognitive processing system.

[1]Because the middle ear is located behind the eardrum and the inner ear is located in the temporal bone, the location of Server 5 is marked outside of the picture of the brain in Fig. 2.

Following Baddeley's working memory model, there are four components in the working memory system: a visuospatial sketchpad (Server A), representing the right-hemisphere posterior parietal cortex; a phonological loop (Server B), standing for the left-hemisphere posterior parietal cortex; a central executor (Server C), representing the dorsolateral prefrontal cortex, the anterior–dorsal prefrontal cortex, and the middle frontal gyrus; and a performance monitor (Server E), standing for the anterior cingulate cortex. The visuospatial sketchpad and the phonological loop store and maintain visuospatial and phonological information in working memory [44].

The goal execution system (Server G) represents the orbitofrontal region, the brain stem including the LC–NE system, and the amygdala complex which are typically involved in goal initiation and motivation [50]. In addition, it sends the neuromodulator entities to other servers following the NE output function in the model of Nieuwenhuis *et al.* [18].

The long-term memory system represents the following two types of long-term memory in the human brain: 1) declarative (facts and events) and spatial memory (Server H), standing for the medial temporal lobe including the hippocampus and the diencephalons which store various kinds of production rules in choice reaction, long-term spatial information, perceptual judgment, decision making, and problem solving; and 2) nondeclarative memory (procedural memory and motor program) (Server D), representing the striatal and cerebellar systems which store all of the steps in a task procedure and the motor programs related to motor execution [20].

The complex cognitive processing system (Server F) stands for the brain areas performing complex cognitive functions—multiple-choice decisions, phonological judgments, spatial working memory operations, visuomotor choices, and mental calculations. These brain areas include the intraparietal sulcus, the superior frontal gyrus, the inferior frontal gyrus, the inferior parietal and ventrolateral frontal cortices, the intraparietal sulcus, and the superior parietal gyrus [44], [51], [52].

C. Motor Subnetwork

The motor subnetwork includes five servers corresponding to the major brain areas in retrieval, assembling, and execution of motor commands as well as sensory information feedback. First, Server V represents the premotor cortex in Brodmann Area 6, which plays an important role in sensorimotor and sensory cue detection [43], [53], [54]. Second, the basal ganglia

(Server W) retrieves motor programs and long-term procedural information from long-term procedural memory (Server D) [20], [55], [56]. Third, the supplementary motor area and the pre-SMA (Server Y) have the major function of assembling motor programs and ensuring movement accuracy [57]. Fourth, the function of the primary motor cortex (Server Z) is to address the spinal and bulbar motor neurons and transmit the neural signals to different body parts as motor actuators (mouth, left and right hand, and left and right foot servers, etc. [43]). Fifth, the S1 (the somatosensory cortex, Server X) collects motor information of efference copies from the primary motor cortex (Server Z) and sensory information from body parts and then relays them to the prefrontal cortex (Server C) as well as the SMA (Server Y) [43].

III. Modeling of Human Performance and P300 in a Tracking Task

In the following section, we describe our use of the queuing network modeling approach to model human performance and P300. First, a set of formulas is developed and implemented in the simulation model to quantify the amplitude and latency of P300. Second, a representative experiment on human performance and P300 is described, which was used to validate the modeling method proposed in this paper. In the third section, we describe how to simulate performance and P300 with QN–MHP.

A. Modeling the Amplitude and Latency of P300

Quantification of P300's amplitude and latency in the queuing network model is composed of the following two parts: 1) modeling the entities representing the neuromodulator in synaptic transmission and 2) based on this modeling result and existing computational models in electric fields of the brain, both the amplitude and latency of P300 are quantified by a set of formulas. All of these formulas are implemented in the simulation model so that the model is able to generate the corresponding values for the dependent variables in real time.

1) Modeling NE in Synaptic Transmission: As described in Section I of this paper, after NE is produced from the LC–NE system, NE reaches the target brain regions and is involved in processing the information of tasks [88], [92]. Based on the balance of NE before and after synaptic transmission [19], [20], the total amount of released NE in processing the tasks (supposedly, there are ξ tasks which are concurrently processed) equals the difference between the amount of NE synthesized from the LC–NE system ($\mathrm{NE_{LC}}$ [18], [68]) and the amount of residual NE left ($\mathrm{NE_0}$) in the presynaptic neurons [see (1)], where τ is a normally distributed random factor with mean being equal to zero

$$\sum_{m=1}^{\xi} \mathrm{NE}_{\mathrm{rel},m} = \mathrm{NE_{LC}} - \mathrm{NE_0} + \tau. \tag{1}$$

For any one of these ξ tasks, the amount of NE released for task $i(\mathrm{NE}_{\mathrm{rel},i})$ is determined by

$$\mathrm{NE}_{\mathrm{rel},i} = \sum_{m=1}^{\xi} \mathrm{NE}_{\mathrm{rel},m} - \sum_{m\neq i}^{\xi} \mathrm{NE}_{\mathrm{rel},m}. \tag{2}$$

Therefore, we have

$$\mathrm{NE}_{\mathrm{rel},i} = \mathrm{NE_{LC}} - \sum_{m\neq i}^{\xi} \mathrm{NE}_{\mathrm{rel},m} - \mathrm{NE_0} + \tau. \tag{3}$$

Equation (3) can be rewritten as

$$\mathrm{NE}_{\mathrm{rel},i} = \mathrm{NE_{LC}} - \sum_{m\neq i}^{\xi} \sum_{\text{all } j} N_{m,j} C_{m,j} \mathrm{NE}_p - \mathrm{NE_0} + \tau \tag{4}$$

where $N_{m,j}$ is the number of information entities of other tasks concurrently processed in server j, $C_{m,j}$ is the number of processing cycles for each of those entities at server j, and NE_p is the amount of NE needed for each of those entities at each processing cycle at server j.

2) Modeling P300 Amplitude: In the computational models of brain potentials, Nunez [63] proposed the following basic formula for quantifying the amplitude of the brain potentials:

$$\phi = \frac{I}{4\pi r \delta} \tag{5}$$

where ϕ is the amplitude of the ERP potential (in microvolts), r is the distance from the electrical field point (the location where NE is released) to locations of the electrodes on the scalp, δ is the resistivity of the brain regions across this distance, and I is the current from the electrical field point where NE is released.

Because there is an inversely proportional relation between the resistance and the amount of NE released $(\mathrm{NE_{rel}})$ [18], [64], δ in (5) can be further quantified in (6) where b is a constant in this inverse relationship

$$\delta = b/\mathrm{NE_{rel}}. \tag{6}$$

Moreover, the number of population spike trains (represented by information entities) (N) is in direct proportion to the current [63]. I in (5) can be quantified in (7) where k is a constant in this relationship

$$I = kN. \tag{7}$$

Combining (5)–(7), we have

$$\phi = \frac{kN}{4\pi r(b/\mathrm{NE_{rel}})} = (k/b)\frac{\mathrm{NE_{rel}} N}{4\pi r}. \tag{8}$$

Furthermore, because P300 comes from the generators of P300 wave in certain brain regions, (4) can be further developed into

$$\mathrm{NE}_{\mathrm{rel},i} = \mathrm{NE_{LC}} - \sum_{m\neq i}^{\xi} \sum_{\text{all } j'} N_{m,j'} C_{m,j'} \mathrm{NE}_p - \mathrm{NE_0} + \tau \tag{9}$$

where j' represents the servers which can serve as the generators of P300 corresponding to the neuroscience findings (servers in the perceptual subnetwork; Servers A, B, C, E, and F in the cognitive subnetwork corresponding to the P300 generators described in Section I).

TABLE I
NGOMSL-STYLE TASK DESCRIPTION OF THE MANUAL TRACKING AND AUDITORY PROBE COUNTING TASKS

GOAL: Do manual tracking task	GOAL: Do auditory probe counting task
Method for GOAL: Do manual tracking task	Method for GOAL: Do auditory probe counting task
Step 1. Watch for <the spatial difference between the cursor and the target> on <the display>	Step 1. Listen to <the tone> from <the speaker>
Step 2. Retain < the spatial difference>	Step 2. Retain <the tone>
Step 3. Decide: if there is a difference then go to step 4; else go to step 7	Step 3. Compare: <the tone> with <the target tone> in memory
Step 4. Compute <the expected movement direction (θ) and time of the joystick (t)>	Step 4. Decide: If match, then go to step 5
Step 5. Move <joystick> in <direction θ> for time <t>	Else move to step 1
Step 6. Go to step 1	Step 5. Compute <increase the counter>
Step 7. Stop moving <joystick>	Step 6. Retain <the counter>

By combining (8) and (9), the P300 amplitude, including its peak for task i, is quantified in

$$\phi_i = (k/b)\frac{\mathrm{NE}_{\mathrm{rel},i}N_i}{4\pi r} = (k/b)\frac{N_i}{4\pi r}\left(\mathrm{NE}_{\mathrm{LC}} - \sum_{m\neq i}^{\xi}\sum_{\text{all } j'} N_{m,j'}C_{m,j'}\mathrm{NE}_p - \mathrm{NE}_0 + \tau\right). \quad (10)$$

Therefore, when the amount of NE used by the primary task increases from zero (single-secondary-task condition) to a certain value (dual-task condition), the amount of NE available for the secondary tasks decreases. This decrease in the amount of NE produces an increase in the resistivity of the brain regions and then a decrease in the amplitude of P300 of the secondary task. The P300 amplitude of the secondary task reduces further as the difficulty of the primary task increases, consuming a greater amount of NE.

3) Modeling P300 Latency: The latency of P300 for a certain task $i(L_i)$ is composed of the following three parts: the time interval between the stimulus presentation and the arrival of stimulus information at the LC–NE system $(T_{i,P} + T_{i,A/B} + T_{i,C} + T_{i,E})$, the time interval between the arrival of stimulus information at the LC–NE system $(t = 0)$ and the time point when $\mathrm{NE}_{\mathrm{LC}}$ reaches its peak (t_p), and the conduction time of NE from LC to the forebrain $(\mathrm{NE}_{\mathrm{cond}})$ which processes task information, as shown in

$$L_i = T_{i,P} + T_{i,A/B} + T_{i,C} + T_{i,E} + t_p + NE_{\mathrm{cond}} \quad (11)$$

where $T_{i,P}$, $T_{i,A/B}$, $T_{i,C}$, and $T_{i,E}$ are the processing times of task i at the perceptual subnetwork, at Server A or B, and at Servers C and E, respectively.

B. Representative Experiment on P300 and Human Performance

Wickens *et al.* [14] measured human performance and the P300 in a concurrent task which includes a visual–manual tracking task (primary task) and an auditory probe counting task (secondary task). In the primary task, subjects manipulated a joystick and attempted to superimpose a cursor on a target which was moving in a series of discrete horizontal displacement on a visual display. The following were the three levels of difficulty in the primary task. 1) First-order predictable (1P): The target moved only in a left–right direction, and only the magnitude of the movement/step was unpredictable; the control of the cursor with the joystick followed first-order control—constant displacement of the joystick caused the cursor to move at a constant velocity in the movement direction of the joystick. 2) First-order unpredictable (1U): Both direction and magnitude of the movement of the target were unpredictable, and the control of the cursor with the joystick still followed first-order control. 3) Second-order unpredictable (2U): Both direction and magnitude of the movement of the target were unpredictable, and the control of the cursor with the joystick followed second-order control—constant displacement of the joystick accelerated the cursor's movement. Concurrently with the tracking tasks, the subjects were assigned to perform an auditory probe counting task. The subjects heard a Bernoulli series of tones of high and low pitches, occurring with equal probability, and the subjects were instructed to count the number of occurrences of the low-pitched tones. They found that the P300 amplitude (peak value) of the secondary task was reduced in dual-task conditions compared with that in a single-task situation and that the P300 amplitude (peak value) was decreased further when the difficulty of the primary task increased.

C. Simulation of Human Performance in the Target Experiment

Simulation of any human–machine interaction task requires the specification of the following three components: a human model, the machine or the environment with which the human model interacts, and the task input to the human model. These three components correspond to the simulation model of queuing network (QN–MHP), a joystick, a visual display presenting the cursor and the target, and a speaker presenting the auditory stimuli, respectively, in the context of the dual task—manual tracking and auditory probe counting (see Fig. 2).

The general human model of QN–MHP is described in the previous section. In order to possess the basic knowledge of how to track and count, the QN–MHP must have the corresponding procedure knowledge rules stored in its long-term procedure memory server. Thus, following the general method of QN–MHP simulation [61], the NGOSML-style (an acronym for a Natural Language GOMS: Goals, Operators, Methods, and Selection rules) task descriptions of both the manual tracking and auditory probe counting tasks are developed (see Table I) and stored in server D as the long-term procedure knowledge of the task in the model. For the tracking task, first, the model watches for the spatial difference between the cursor and the target. Second, if there is a difference, the model computes the expected movement time (1P, 1U, and 2U

conditions) and expected movement direction (1U and 2U conditions) (with an increase in tracking difficulty, the number of cycles in computation increases). Third, the model executes the movement to move the joystick in the expected movement direction and time. Similarly, in the auditory probe counting task, the model increases the value of a counter if it receives a target low-pitch tone from the auditory perceptual subnetwork. All of these steps or operators are defined in a task-independent manner, with the task-specific information being treated as their parameters.

More importantly, one of the unique features of QN–MHP in modeling concurrent tasks is that the entities representing the information of the two tasks can be processed in the network concurrently, and multitask performance emerges as the behavior of multiple streams of information flowing through a network without writing another program to either interleave two-task procedures into a serial program or control the two-task procedure with an executive control [61].

In addition, to define the joystick with which the QN–MHP interacts, a software module called m-hJOYSTICK is implemented to represent the joystick in the tracking task. This module defines the order of control (first or second order), collects the movement information of the hand server, and transmits the corresponding position of the cursor on the visual display which is implemented in a server in the model (see Fig. 2). This module also computes and records the root-mean-square (rms) error of the tracking task. Another software module is implemented to represent the speaker which produces the entities of auditory stimuli and supplies them to the auditory perceptual subnetwork. Human performance is generated by a natural interaction of the entities of the concurrent tasks being processed in the network following the task descriptions (see Fig. 2).

IV. Simulation Results and Their Validation

By implementing the equations developed in the previous section into the simulation model (see Appendix I for values of several parameters in these equations), the simulation results are obtained and compared with the target experimental results of Wickens *et al.* [14].

Fig. 3 shows the simulation results of the rms error of human performance in comparison with experimental results. The R square of the model is 0.99, and rms equals 13.24 [comparison between single and dual tasks, Fig. 3(a)]; the R square is 0.95, and rms equals 131.6 [comparison among three difficulty levels, Fig. 3(b)].

The latency and the amplitude of P300 (peak value) are shown in Figs. 4 and 5, respectively. For the latency, R square $=$ 0.99, and rms $= 1$; for the amplitude, R square $= 0.99$, and rms $= 0.39$. The P300 amplitudes (peak values) of the secondary task, as shown in Fig. 5, are smaller in the dual-task condition than in the single-task condition (R square $= 0.99$ and rms $= 0.39$).

Fig. 6 shows a comparison of the real-time change of the P300 amplitude of the secondary task in the experiment of Wickens *et al.* and the simulation results (secondary task only and dual-task conditions). In the single-task condition (secondary task only), the R square of the model is 0.93, and rms equals 1.63; in the concurrent-task condition, the R square of the model is 0.86, and rms equals 1.66.

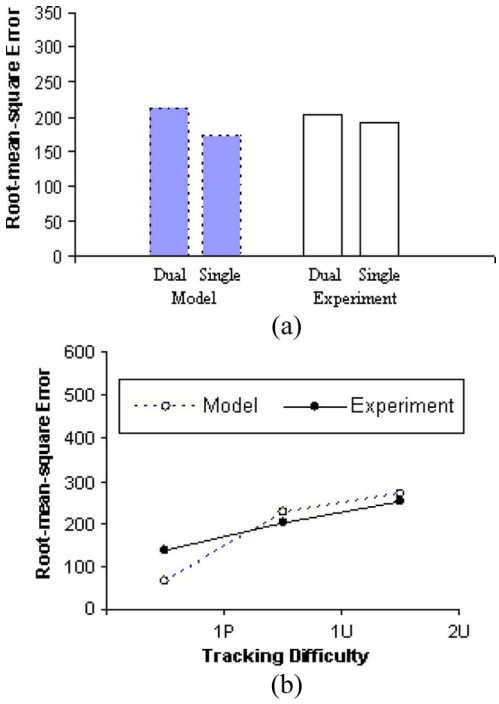

Fig. 3. (Solid lines) RMS error in the study of Wickens *et al.* [14] in comparison with (dashed lines) the queuing network simulation results. (a) Comparison between single (secondary task only) and dual tasks. (b) Comparison between the three difficulty levels.

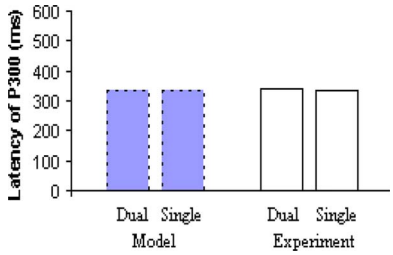

Fig. 4. (Solid lines) P300 latency in the study of Wickens *et al.* [14] in comparison with (dashed lines) the queuing network simulation results (single: secondary task only; dual: concurrent task).

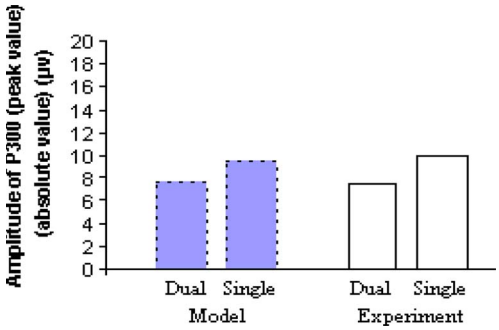

Fig. 5. (Solid lines) P300 amplitude (peak value) in the study of Wickens *et al.* [14] in comparison with (dashed lines) the queuing network simulation results (single: secondary task only; dual: concurrent task).

The change of the P300 amplitude (peak value) of the secondary task with an increase of tracking difficulty in the primary task is shown in Fig. 7. The R square of the model is 0.99, and rms equals 5.86.

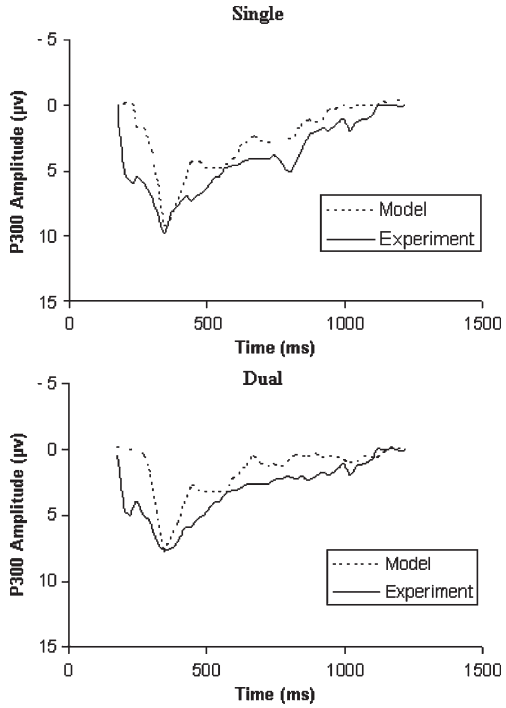

Fig. 6. (Solid lines) Real-time P300 amplitude in the study of Wickens *et al.* [14] in comparison with (dashed lines) the queuing network simulation results (single: secondary task only; dual: concurrent task).

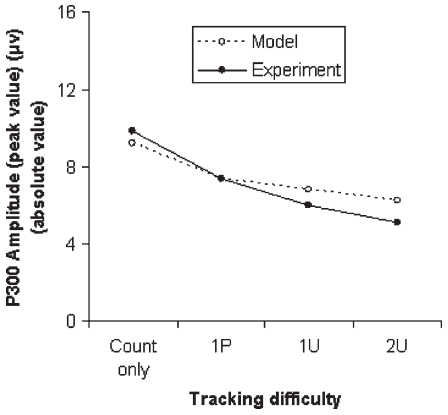

Fig. 7. (Solid lines) Change of P300 amplitude (peak value) with an increase of tracking difficulty in the study of Wickens *et al.* [14] in comparison with (dashed lines) the queuing network simulation results.

V. Extension and Application of the Model

Equations developed in this paper can be extended further to account for other P300 studies in multitasking and can be used in designing user interface in dual tasks, including designing the stimuli or representation of multiple tasks on user interface and determining the maximal difficulty level of a task in multitasking.

Based on (11), the P300 amplitude of Task 2 can be quantified into

$$\phi_2 = (k/b)\frac{\mathrm{NE}_{\mathrm{rel},i}N_i}{4\pi r} = (k/b)\frac{N_2}{4\pi r} \times \left(\mathrm{NE}_{\mathrm{LC}} - \sum_{m\neq i}^{\xi}\sum_{\text{all } j'} N_{1,j'}C_{1,j'}\mathrm{NE}_p - \mathrm{NE}_0 + \tau\right). \quad (12)$$

If there are only two tasks, (12) can be simplified into

$$\phi_2 = (k/b)\frac{N_2}{4\pi r}\left(\mathrm{NE}_{\mathrm{LC}} - \sum_{\text{all } j'} N_{1,j'}C_{1,j'}\mathrm{NE}_p - \mathrm{NE}_0 + \tau\right) = \frac{(k/b)}{4\pi r}N_2\left(-\sum_{\text{all } j'} N_{1,j'}C_{1,j'}\mathrm{NE}_p + \mathrm{NE}_{\mathrm{LC}} - \mathrm{NE}_0 + \tau\right). \quad (13)$$

Because $\sum_{\text{all}j'} N_{1,j'}C_{1,j'} = \mathrm{NE}_p \sum_{\text{all}j'} N_{1,j'}C_{1,j'} = \mathrm{NE}_p n_1 \overline{N_1 C1}$, where $\overline{N_1}$ and $\overline{C_1}$ are the averaged number and cycle times of entities of Task 1 in the network, respectively (n_1 is the number of servers processing entities of Task 1)

$$\begin{aligned}\phi_2 &= \frac{(k/b)}{4\pi r}(\alpha\overline{N_1} + \beta)(-\mathrm{NE}_p n\overline{N_1 C_1} + \mathrm{NE}_{\mathrm{LC}} - \mathrm{NE}_0 + \tau)\\ &= 0.76(\alpha\overline{N_1} + \beta)(-0.63n\overline{N_1 C_1} + \mathrm{NE}_{\mathrm{LC}} - 0.38),\\ &\qquad (\text{assuming that } \tau = 0 \text{ on average}). \end{aligned} \quad (14)$$

Similarly

$$\phi_1 = \frac{(k/b)}{4\pi r}N_1(-\mathrm{NE}_p n_2\overline{N_2 C_2} + \mathrm{NE}_{\mathrm{LC}} - \mathrm{NE}_0 + \tau). \quad (15)$$

Equations (14) and (15) can be used to optimize dual-task performance in various domains. First, because P300 amplitude is one of the indexes to reflect the resource available for a task, (14) and (15) can help us identify the critical factors in maximizing the resource of Tasks 1 and 2 in dual tasks: N_2, $\overline{C_1}$, $\overline{N_1}$, n_1, and $\mathrm{NE}_{\mathrm{LC}}$ to maximize the resource of Task 2; N_1, $\overline{C_2}$, $\overline{N_2}$, n_2, and $\mathrm{NE}_{\mathrm{LC}}$ to maximize the resource of Task 1. Second, to maximize the resource of Task 2, N_2 and $\overline{N_1}$ can be optimized by properly designing the stimuli of the two tasks according to (14); n_1 and $\overline{C_1}$ can be reduced by practicing Task 1. The same logic can also be applied to maximize the resource to Task 1. Third, (14) and (15) can help us quantify the maximal difficulty level of a task in multitasking so that the resource available for the other task is maintained above the minimal level. In this paper, we focus our discussion on the following: 1) how to quantify the relation between N_2 and $\overline{N_1}$ with its implication in designing stimuli in multitasking and 2) how to quantify the maximal difficulty level of a task so that the resource available for the other task is above the minimal level.

1) Relation Between N_2 and $\overline{N_1}$ With Its Implication in Interface Design in Multitasking: Suppose there is a directly proportional relation between N_2 and $\overline{N_1}$

$$N_2 = \alpha\overline{N_1} + \beta. \quad (16)$$

Then

$$\begin{aligned}\phi_2 &= \frac{(k/b)}{4\pi r}(\alpha\overline{N_1} + \beta)(-\mathrm{NE}_p n_1\overline{N_1 C_1} + \mathrm{NE}_{\mathrm{LC}} - \mathrm{NE}_0 + \tau)\\ &= 0.76(\alpha\overline{N_1} + \beta)(-0.63n_1\overline{N_1 C_1} + \mathrm{NE}_{\mathrm{LC}} - 0.38),\\ &\quad (\text{assuming that } \tau = 0 \text{ on average})\\ &= -0.48n_1\alpha\overline{C_1 N_1}^2\\ &\quad + \left(-0.48n_1\beta\overline{C_1} + 0.76\alpha\mathrm{NE}_{\mathrm{LC}} - 0.29\alpha\right)\overline{N_1}\\ &\quad + 0.76\beta(\mathrm{NE}_{\mathrm{LC}} - 0.38). \end{aligned} \quad (17)$$

In addition, according to the properties in queuing networks, there is an inversely proportional relation between the difficulty level of Task 1 (TD_1) and $\overline{N_1}$, as well as a directly proportional relation between TD_1 and $\overline{C_1}$

$$\mathrm{TD}_1 = -g\overline{N_1} + h, \qquad (g > 0; \quad h > g\overline{N_1}) \tag{18}$$

$$\mathrm{TD}_1 = s\overline{C_1} + t, \qquad (s > 0; \quad t = 0 \text{ when } \overline{C_1} = 0,\ \mathrm{TD}_1 = 0). \tag{19}$$

By combining (17)–(19), (17) can be further developed into

$$\begin{aligned}\phi_2 = {} & -0.48 n_1 \alpha s^{-1} g^{-2} \mathrm{TD}_1^3 \\ & + \left(0.96 h n_1 \alpha s^{-1} g^{-2} + 0.48 n_1 \beta s^{-1} g^{-1}\right) \mathrm{TD}_1^2 \\ & + \left(-0.48 n_1 \alpha s^{-1} g^{-2} h^2 - 0.76 \alpha g^{-1} \mathrm{NE_{LC}} \right. \\ & \quad \left. + 0.29 \alpha g^{-1} - 0.48 n_1 \beta h s^{-1} g^{-1}\right) \mathrm{TD}_1 \\ & + 0.76 \alpha h g^{-1} \mathrm{NE_{LC}} - 0.29 \alpha h g^{-1} + 0.76 \beta (\mathrm{NE_{LC}} - 0.38).\end{aligned} \tag{20}$$

Take partial derivative

$$\begin{aligned}\frac{\partial \phi_2}{\partial \mathrm{TD}_1} = {} & -1.44 n_1 \alpha s^{-1} g^{-2} \mathrm{TD}_1^2 \\ & + \left(1.92 h n_1 \alpha s^{-1} g^{-2} + 0.96 n_1 \beta s^{-1} g^{-1}\right) \mathrm{TD}_1 \\ & + \left(-0.48 n_1 \alpha s^{-1} g^{-2} h^2 - 0.76 \alpha g^{-1} \mathrm{NE_{LC}} \right. \\ & \quad \left. + 0.29 \alpha g^{-1} - 0.48 n_1 \beta h s^{-1} g^{-1}\right).\end{aligned} \tag{21}$$

Based on (21), depending on the value of α, β, and other parameters, an increase of Task 1 difficulty level may generate an increase of ϕ_2, a decrease of ϕ_2, or no change of ϕ_2 (see Fig. 8 and Appendix II for equations A)–E) including their solutions).

Based on the derivation results of (21) in Appendix II, Fig. 9 provides a more intuitive illustration of Conditions 1) and 2) in Fig. 8, connecting the relation between N_2 and $\overline{N_1}$ and the change of ϕ_2: 1) If there is an inversely proportional relation between N_2 and N_1 bar ($\overline{N_1}$) (e.g., $\alpha = -1$), the greater the number of Task 1 ($\overline{N_1}$) entities on average, the less the number of Task 2 (T2) entities processed in the network; (21) predicts an increase of the P300 amplitude (resource) of T2 (see Condition 1) in Fig. 9); 2) if there is a directly proportional relation between N_2 and N_1 bar ($\overline{N_1}$) (e.g., $\alpha = 1$), the less number of Task 1 ($\overline{N_1}$) on average, the less number of Task 2 (T2) entities processed in the network; (21) predicts a decrease of the P300 amplitude (resource) of T2 (see Condition 2) in Fig. 9).

The predicted results in Fig. 9 are consistent with the existing results in ERP studies [65]. In the study of Kramer *et al.* [65], when the stimuli of the primary task (T1) and the secondary task (T2) are integrated into the same stimuli (T1: tracking a moving object; T2: counting the transitional change of the same moving object) ("Dual-Task Integrality Condition" in [65, Fig. 1]), the amplitude of P300 of T2 increases with an increase of the difficulty level of T1. Different from the study of Wickens *et al.* [14] in which the stimuli of T1 and T2 are not in the same object, "the dual-task integrality" condition in the study of Kramer *et al.* sets the stimuli of T1 and T2 into the properties of the same object. In QN–MHP, this setting of the experiment is represented as using one type of entity (called "shared entity" here) with different attributes. In other words, one entity carries

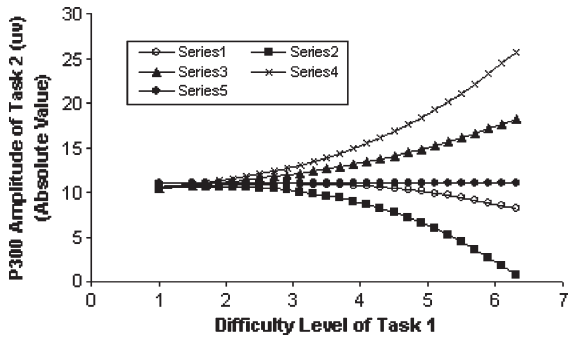

Fig. 8. Three conditions relating the difficulty level of Task 1 and the change of ϕ_2. Condition 1): An increase of the difficulty level of Task 1 (TD_1) will increase the value of ϕ_2 (Series 3 and 4, $\alpha_4 < \alpha_3 < \Gamma$). Condition 2): An increase of the difficulty level of Task 1 (TD_1) will decrease the value of ϕ_2 (Series 1 and 2, $\alpha_2 > \alpha_1 > \Gamma$). Condition 3): An increase of the difficulty level of Task 1 (TD_1) does not affect the value of ϕ_2 (Series 5, $\alpha_5 = \Gamma$).

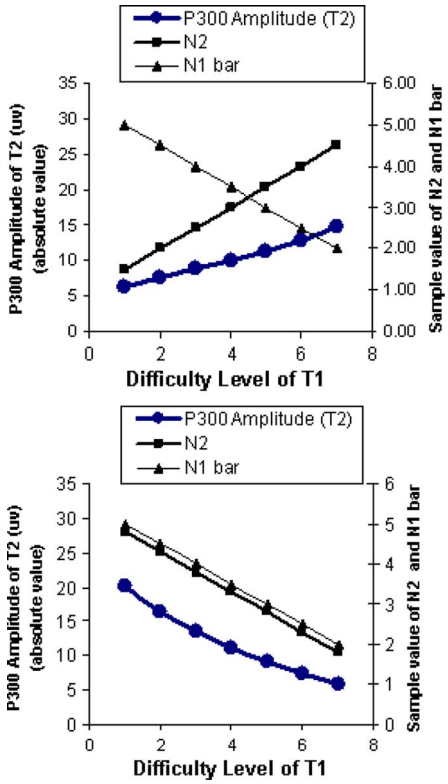

Fig. 9. Effect of the relationship between N_2 and $\overline{N_1}$ on the change of the P300 amplitude of Task 2 with an increase of the difficulty level of Task 1. Condition 1): An inverse relation between N_2 and $\overline{N_1}$ produced an increase ϕ_2 with an increase of the difficulty level of Task 1 (TD_1) ($\alpha = -1 < \Gamma$). Condition 2): A direct relation between N_2 and $\overline{N_1}$ produced a decrease of ϕ_2 with an increase of the difficulty level of Task 1 (TD_1) ($\alpha = 1 > \Gamma$).

the two tasks' information at the same time, generating parallel processing in the perceptual subnetwork in the model. When the difficulty level of T1 increases, the shared entities of T1 and T2 stay for a longer time at Server F to process the information of T1 (lower value of $\overline{N_1}$), increasing the number of shared entities in the other servers in the cognitive subnetwork and the perceptual subnetwork. Because the shared entities also carry the information of T2, more information of T2 gets processed at the same time while the shared entities are waiting longer for

the service of Server F (higher value of N_2). For explanation purposes, by inserting the value of other parameters, (13) can be simplified into

$$\begin{aligned}\phi_2 &= \frac{(k/b)}{4\pi r} N_2 \left(-\mathrm{NE}_p n\overline{N_1 C_1} + \mathrm{NE}_{\mathrm{LC}} - \mathrm{NE}_0 + \tau\right) \\ &= 0.76 N_2 \left(-0.75\overline{N_1 C_1} + 1.62\right) \\ &= 1.215 N_2 - 0.57\overline{N_1 C_1}. \end{aligned} \tag{22}$$

In (22), the constant before N_2 is greater than that in front of $\overline{N_1 C_1}$; therefore, the value of N_2 becomes the major factor determining the value of ϕ_2. A higher value of N_2 in the same object condition increases the value of ϕ_2.

In contrast, if the stimuli of T1 and T2 are not set in the same object (e.g., in [14] or the different object condition in [65]), they are represented as two types of entities in the network. When the difficulty level of T1 increases, the entities of T1 spend more time at Server F in the cognitive subnetwork (lower value of $\overline{N_1}$), decreasing the number of entities of T2 receiving the service of Server F (lower value of N_2) and the value of ϕ_2 [see (22)].

The quantification of the relationship between N2 and $\overline{N_1}$ on the change of the P300 amplitude of Task 2 earlier can be applied in designing user interfaces in multitasking. First, based on Figs. 8 and 9 and (13), it is recommended that the information of T1 and T2 be encoded into the same object or stimuli, creating the inverse relation between N_2 and $\overline{N_1}$ with an increase of the T1 difficulty level and maximizing the parallel processing of information of T2 when the processing of T1 is delayed. Moreover, as long as the derived α is lower than the threshold (Γ) derived in Appendix II, an increase of the T1 difficulty level will increase the value of ϕ_2 as an indication of the resource available for Task 2; the lower the value of α, the more resources are available for Task 2. Second, in circumstances where the stimuli of the two tasks cannot be set in the same object, one of the focuses of the designer is to lower the derived α so that its value will be closer to Γ; the higher the value of α, the less resources are available for Task 2 when the difficulty level of Task 1 increases.

To implement this in real user interface design, first, a similar simulation process described in this paper is needed to obtain the value of α and other parameters in Appendix II (see [61], [83], and [84] for a detailed description about how to use QN–MHP to simulate other tasks). Second, the value of the threshold (Γ) can be obtained via equations A)–D) and their solutions in Appendix II. Third, the original design of user information can be revised (e.g., integrating the information of the two tasks in the same object or reducing the distance between the locations of the two objects belonging to T1 and T2) until the value of α_1 is lower than Γ in the same object condition (the lower, the better) or α_1 is closer to Γ in the different object condition (the closer, the better). The same logic can also be applied to the situation wherein the resource of Task 1 is to be maximized when the difficulty level of Task 2 increases.

2) Quantification of the Maximal Difficulty Level of a Task in Multitasking: Equation (17) can also be used to determine the maximal difficulty level of a task in multitasking. Suppose a minimal level of resource for task i is needed (for example, $\phi_{i\,\min}$ found by ERP experiments), (17) can be generalized into

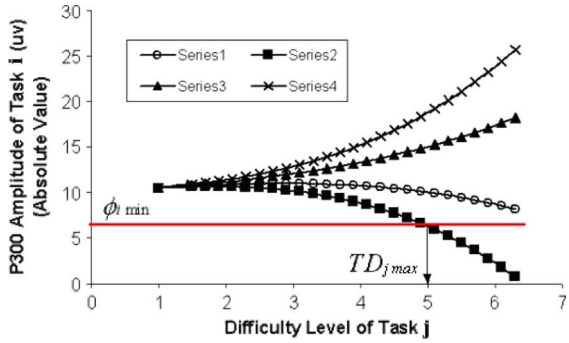

Fig. 10. Deriving the maximal task difficulty level $(\mathrm{TD}_{j\,\max})$ using (23).

(23) to quantify the maximal difficulty level of the other task $j(\mathrm{TD}_{j\,\max})$ [see Fig. 10 as an illustration of (23)]

$$\begin{aligned}\phi_{i}\,\min = & -0.48 n_j \alpha s^{-1} g^{-2} \mathrm{TD}_{j\,\max}^3 \\ & + \left(0.96 h n_j \alpha s^{-1} g^{-2} + 0.48 n_j \beta s^{-1} g^{-1}\right) \mathrm{TD}_{j\,\max}^2 \\ & + \left(-0.48 n_j \alpha s^{-1} g^{-2} h^2 - 0.76 \alpha g^{-1} \mathrm{NE}_{\mathrm{LC}}\right. \\ & \quad \left. + 0.29 \alpha g^{-1} - 0.48 n_j \beta h s^{-1} g^{-1}\right) \mathrm{TD}_{j\,\max} \\ & + 0.76 \alpha h g^{-1} \mathrm{NE}_{\mathrm{LC}} - 0.29 \alpha h g^{-1} \\ & + 0.76 \beta (\mathrm{NE}_{\mathrm{LC}} - 0.38). \end{aligned} \tag{23}$$

For example, in a driving task, suppose T1 is steering a vehicle on a highway and T2 is operating an in-vehicle device, and we have obtained the minimal value of $\phi_1(\phi_{1\,\min})$ based on existing ERP experiments in driving. After performing similar simulation using the current model (see [61], [83], and [84] for a detailed description on how to use QN–MHP to model driving and other tasks), users of the model can obtain the parameter values in (23) except $\mathrm{TD}_{2\,\max}$. Finally, the maximal task difficulty level of T2 $(\mathrm{TD}_{2\,\max})$ can be obtained via (23); and it can be used as a guideline to design the user interface of an in-vehicle device, so that operating this device while, at the same time, driving will not exceed the "red line" of resource for the primary driving task.

VI. Conclusion

We described a queuing network modeling approach to model human performance and P300, including its latency, amplitude, and real-time change of amplitude simultaneously in dual-task situations. It not only successfully accounts for one of the major findings in measuring mental workload found by Wickens *et al.* but also provides a quantitative explanation why, in different experimental settings, the P300 amplitude of a secondary task may either decrease [14] or increase [65] in dual-task conditions when the difficulty of the primary task is higher. By quantifying these major findings, QN–MHP also offers a quantitative mechanism with corresponding neurological support to explain how these ERP phenomena are produced in the human brain as an attempt to meet requirements both for engineering applications and biological realism. This queuing network modeling approach demonstrates its value in describing and predicting behavioral performance and the important aspects of the macroscopic electrical brain activities.

In modeling the experimental results of the study of Wickens *et al.* [14], the simulation mechanism of the queuing

network modeling approach is consistent with existing models of mental workload and the results of other experimental studies. First, for the conceptual model proposed by Wickens [22], the queuing network modeling approach finds a potential neurological basis for the concept of "resource" in Wickens' model. In a certain period, the amount of NE synthesized in the brain is constrained by the amount of tyrosine, dopa, and energy (adenosine triphosphate) in the neurological system [19]. As the demand for NE by the primary task increases, the available amount of NE for the secondary task decreases naturally. This decrease in the available NE produces an increase in the resistivity of the brain regions and then decreases the amplitude of P300 measured by the ERP techniques. Second, the modeled P300 latency [see (11)] is composed of the processing of entities at the perceptual and cognitive subnetworks, which is also consistent with Wickens' model in that the latency of P300 results from the perceptual and cognitive processing activities before the motor response stage [22].

Another potential contribution of this paper is that the mathematical equations developed can be extended further to account for other P300 studies in multitasking with its application in multitask user interface design. The extension of the model is able to account for different patterns of P300 in different experimental settings, including an increase, decrease, or no change in P300 when the task difficulty changes. The computational model can unify several important findings in P300 studies [14], [65]. In addition, the computational model can also be used in designing user interface in dual tasks by determining the degree of information integration of the two tasks in the same object and setting the maximal task difficulty level.

The current modeling approach provides a useful connection between neuron activity, mental workload, and human performance. It uses both bottom–up and top–down modeling methods. The quantification of NE in synaptic transmission in the model is a bottom–up modeling process starting from microactivities in the brain, whereas the quantification of task procedures and a task-independent queuing network structure of brain regions is a top–down modeling. Moreover, the current model incorporates the NE output of the neural network model of the LC–NE system [18], offering a useful interface between neural network and queuing network models.

Aside from its role in connecting neural network with queuing network models, this queuing network model is useful in predicting mental workload in real-time engineering applications. First, the consistency between the simulation and experimental results suggests that this modeling approach is able to predict mental workload relatively accurately, both in the temporal dimension, as reflected by the P300 latency, and in the intensity dimension, as indicated by the P300 amplitude. This relative sensitivity to the manipulation of the task difficulty level and the arrival patterns of task information makes the model useful in engineering applications. For example, many intelligent or adaptive driver support and warning systems could benefit from computational workload models for estimating driver workload and proposing actions (e.g., redirecting messages into a voice mailbox [66]) to prevent traffic accidents because collecting ERP signals directly in these real-world systems requires expensive devices. By implementing this computational model into these systems, driver mental workload may be estimated more accurately for predicting when the mental workload may reach a "red-line" level (reflected by certain P300 amplitude), as well as by how much and for how long it exceeds that red line.

Second, unlike the traditional mental workload models, the current modeling approach starts from a task-independent cognitive architecture—QN–MHP which has successfully modeled human performance (e.g., reaction time, response accuracy, and eye movement) of various kinds of tasks. The success of modeling mental workload significantly extends the coverage of the model in engineering applications and allows users of the model to model mental workload and human performance at the same time.

The current modeling approach has its limitations because it is the first step to quantify P300 amplitude and latency in dual-task situations using the queuing network modeling methods. Research has shown that other substances, e.g., acetylcholine, may also affect P300 amplitude [85], [86]; therefore, the current model—using NE to quantify P300 amplitude—is only one of the possible approaches to quantify P300 amplitude in dual tasks. Moreover, unlike some other modeling approaches (e.g., Micro-SAINT and IMPRINT) which have validated their prediction in many real systems and different task settings, the current modeling approach has not validated all of the predictions of the model (e.g., the prediction that a change of task difficulty level may not affect the P300 amplitude).

We are extending the current modeling approach to quantify other important findings in mental workload research. For example, by quantifying subnetwork utilizations, the queuing network model is able to predict the subjective mental workload measured by various workload scales. Overall, the queuing network modeling approach shows potential as a useful modeling method to quantify and predict mental workload, behavioral performance, and electrophysiological phenomena of the cognitive system.

APPENDIX I
SETTING OF PARAMETERS

Parameter setting in simulation: No free parameter is used during the simulation process, and all of the values of parameters come from the original settings of QN–MHP [61] and the existing neuroscience studies (see Table II) (free parameter refers to parameters whose value is adjusted by researchers so that the modeling results fit the experimental results).

The following are descriptions of the parameter setting in Table II.

1) NE_p: Based on [67, Fig. 5], eight spikes are observed when the solution of NE was used. The amount of NE in the solution is 20 μmol, which is multiplied by the concentration of NE ($20/200 = 10\%$; see [67, p. 113] for its solution) and the percentage of NE reaching the target brain (proportion of S4 cell in the brain region (4%); see [67, Fig. 1]). The estimated $NE_p = (20/8) * 10\% * 4\% = 0.01$ μmol.
2) NE_0: According to [69, Fig. 1] (control condition, NE concentration level within 15 min), the amount of residual NE left (NE_0) left in the presynaptic neurons

$$-1.44n_1\alpha s^{-1}g^{-2}\text{TD}_1^2+(1.92hn_1\alpha s^{-1}g^{-2}+0.96n_1\beta s^{-1}g^{-1})\text{TD}_1+(-.48n_1\alpha s^{-1}g^{-2}h^2-0.76\alpha g^{-1}\text{NE}_{\text{LC}}+0.29\alpha g^{-1}-0.48n_1\beta hs^{-1}g^{-1})\geq 0$$

$$\Rightarrow \frac{(1.92hn_1\alpha s^{-1}g^{-2}+0.96n_1\beta s^{-1}g^{-1})+\sqrt{(1.92hn_1\alpha s^{-1}g^{-2}+0.96n_1\beta s^{-1}g^{-1})^2+5.76n_1\alpha s^{-1}g^{-2}(-0.48n_1\alpha s^{-1}g^{-2}h^2-0.76\alpha g^{-1}\text{NE}_{\text{LC}}+0.29\alpha g^{-1}-0.48n_1\beta hs^{-1}g^{-1})}}{2.88n_1\alpha s^{-1}g^{-2}}$$

$$>\text{TD}_1>$$

$$\frac{-(1.92hn_1\alpha s^{-1}g^{-2}+0.96n_1\beta s^{-1}g^{-1})+\sqrt{(1.92hn_1\alpha s^{-1}g^{-2}+0.96n_1\beta s^{-1}g^{-1})^2+5.76n_1\alpha s^{-1}g^{-2}(-0.48n_1\alpha s^{-1}g^{-2}h^2-0.76\alpha g^{-1}\text{NE}_{\text{LC}}+0.29\alpha g^{-1}-0.48n_1\beta hs^{-1}g^{-1})}}{-2.88n_1\alpha s^{-1}g^{-2}}$$

$$\Rightarrow$$

A) $$-\sqrt{(1.92hn_1\alpha s^{-1}g^{-2}+0.96n_1\beta s^{-1}g^{-1})^2+5.76n_1\alpha s^{-1}g^{-2}(-0.48n_1\alpha s^{-1}g^{-2}h^2-0.76\alpha g^{-1}\text{NE}_{\text{LC}}+0.29\alpha g^{-1}-0.48n_1\beta hs^{-1}g^{-1})}$$

$$>(1.92hn_1\alpha s^{-1}g^{-2}+0.96n_1\beta s^{-1}g^{-1})-2.88n_1\alpha s^{-1}g^{-2}\text{TD}_1$$

and

B) $$(1.92hn_1\alpha s^{-1}g^{-2}+0.96n_1\beta s^{-1}g^{-1})-2.88n_1\alpha s^{-1}g^{-2}\text{TD}_1$$

$$<\sqrt{(1.92hn_1\alpha s^{-1}g^{-2}+0.96n_1\beta s^{-1}g^{-1})^2+5.76n_1\alpha s^{-1}g^{-2}(-0.48n_1\alpha s^{-1}g^{-2}h^2-0.76\alpha g^{-1}\text{NE}_{\text{LC}}+0.29\alpha g^{-1}-0.48n_1\beta hs^{-1}g^{-1})} \quad (24)$$

$$\alpha<\frac{\beta(2.77h-5.53\text{TD}_1)}{-2.77g^{-1}h^2-4.38sn_1^{-1}\text{NE}_{\text{LC}}+1.67sn_1^{-1}-8.3g^{-1}\text{TD}_1^2-11.06\text{TD}_1hg^{-1}}=\Gamma \quad (\text{and } \alpha<0) \quad (25)$$

$$-1.44n_1\alpha s^{-1}g^{-2}\mathrm{TD}_1^2+(1.92hn_1\alpha s^{-1}g^{-2}+0.96n_1\beta s^{-1}g^{-1})\mathrm{TD}_1+(-0.48n_1\alpha s^{-1}g^{-2}h^2-0.76\alpha g^{-1}\mathrm{NE}_{\mathrm{LC}}+0.29\alpha g^{-1}-0.48n_1\beta hs^{-1}g^{-1})<0$$

$$\Rightarrow \mathrm{TD}_1>\frac{(1.92hn_1\alpha s^{-1}g^{-2}+0.96n_1\beta s^{-1}g^{-1})+\sqrt{(1.92hn_1\alpha s^{-1}g^{-2}+0.96n_1\beta s^{-1}g^{-1})^2+5.76n_1\alpha s^{-1}g^{-2}(-0.48n_1\alpha s^{-1}g^{-2}h^2-0.76\alpha g^{-1}\mathrm{NE}_{\mathrm{LC}}+0.29\alpha g^{-1}-0.48n_1\beta hs^{-1}g^{-1})}}{2.88n_1\alpha s^{-1}g^{-2}}$$

or

$$\mathrm{TD}_1<\frac{-(1.92hn_1\alpha s^{-1}g^{-2}+0.96n_1\beta s^{-1}g^{-1})+\sqrt{(1.92hn_1\alpha s^{-1}g^{-2}+0.96n_1\beta s^{-1}g^{-1})^2+5.76n_1\alpha s^{-1}g^{-2}(-0.48n_1\alpha s^{-1}g^{-2}h^2-0.76\alpha g^{-1}\mathrm{NE}_{\mathrm{LC}}+0.29\alpha g^{-1}-0.48n_1\beta hs^{-1}g^{-1})}}{-2.88n_1\alpha s^{-1}g^{-2}}$$

$\Rightarrow$

C) $$\sqrt{(1.92hn_1\alpha s^{-1}g^{-2}+0.96n_1\beta s^{-1}g^{-1})^2+5.76n_1\alpha s^{-1}g^{-2}(-0.48n_1\alpha s^{-1}g^{-2}h^2-0.76\alpha g^{-1}\mathrm{NE}_{\mathrm{LC}}+0.29\alpha g^{-1}-0.48n_1\beta hs^{-1}g^{-1})}$$
$$<2.88n_1\alpha s^{-1}g^{-2}\mathrm{TD}_1-(1.92hn_1\alpha s^{-1}g^{-2}+0.96n_1\beta s^{-1}g^{-1})$$

or

D) $$(1.92hn_1\alpha s^{-1}g^{-2}+0.96n_1\beta s^{-1}g^{-1})-2.88n_1\alpha s^{-1}g^{-2}\mathrm{TD}_1$$
$$>\sqrt{(1.92hn_1\alpha s^{-1}g^{-2}+0.96n_1\beta s^{-1}g^{-1})^2+5.76n_1\alpha s^{-1}g^{-2}(-0.48n_1\alpha s^{-1}g^{-2}h^2-0.76\alpha g^{-1}\mathrm{NE}_{\mathrm{LC}}+0.29\alpha g^{-1}-0.48n_1\beta hs^{-1}g^{-1})}$$

$$\alpha>\frac{\beta(2.77h-5.53\mathrm{TD}_1)}{-2.77g^{-1}h^2-4.38sn_1^{-1}\mathrm{NE}_{\mathrm{LC}}+1.67sn_1^{-1}-8.3g^{-1}\mathrm{TD}_1^2-11.06\mathrm{TD}_1hg^{-1}}=\Gamma\quad(\text{and }\alpha>0)\tag{26}$$

$$-1.44n_1\alpha s^{-1}g^{-2}\mathrm{TD}_1^2+(1.92hn_1\alpha s^{-1}g^{-2}+0.96n_1\beta s^{-1}g^{-1})\mathrm{TD}_1$$
$$+(-0.48n_1\alpha s^{-1}g^{-2}h^2-0.76\alpha g^{-1}\mathrm{NE}_{\mathrm{LC}}+0.29\alpha g^{-1}-0.48n_1\beta hs^{-1}g^{-1})=0$$

$$\Rightarrow \mathrm{TD}_1=\frac{-(1.92hn_1\alpha s^{-1}g^{-2}+0.96n_1\beta s^{-1}g^{-1})\pm\sqrt{(1.92hn_1\alpha s^{-1}g^{-2}+0.96n_1\beta s^{-1}g^{-1})^2+5.76n_1\alpha s^{-1}g^{-2}(-0.48n_1\alpha s^{-1}g^{-2}h^2-0.76\alpha g^{-1}\mathrm{NE}_{\mathrm{LC}}+0.29\alpha g^{-1}-0.48n_1\beta hs^{-1}g^{-1})}}{-2.88n_1\alpha s^{-1}g^{-2}}$$

$\Rightarrow$

E) $$(1.92hn_1\alpha s^{-1}g^{-2}+0.96n_1\beta s^{-1}g^{-1})^2+5.76n_1\alpha s^{-1}g^{-2}(-0.48n_1\alpha s^{-1}g^{-2}h^2-0.76\alpha g^{-1}\mathrm{NE}_{\mathrm{LC}}+0.29\alpha g^{-1}-0.48n_1\beta hs^{-1}g^{-1})$$
$$=\left[2.88n_1\alpha s^{-1}g^{-2}\mathrm{TD}_1-(1.92hn_1\alpha s^{-1}g^{-2}+0.96n_1\beta s^{-1}g^{-1})\right]^2\tag{27}$$

$$\alpha=\frac{\beta(2.77h-5.53\mathrm{TD}_1)}{-2.77g^{-1}h^2-4.38sn_1^{-1}\mathrm{NE}_{\mathrm{LC}}+1.67sn_1^{-1}-8.3g^{-1}\mathrm{TD}_1^2-11.06\mathrm{TD}_1hg^{-1}}=\Gamma\tag{28}$$

TABLE II
PARAMETERS USED IN SIMULATION

Parameter	Value	Description	Source
$T_{i,AP}$, $T_{i,VP}$	126 ms	Time for auditory or visual perception (1 cycle is 42 ms at each server in perceptual subnetwork)	[62]
$T_{i,A}$, $T_{i,B}$, $T_{i,C}$, $T_{i,E}$, $T_{i,F}$	18 ms	1 processing cycle time at servers in cognitive subnetwork	[62]
$T_{i,W}$, $T_{i,Y}$, $T_{i,Z}$, $T_{i,X}$,	24 ms	1 processing cycle time at servers in motor subnetwork	[62]
NE_p	0.01 μmol	Amount of NE needed for each of those entities at each processingcycle at server j	[68]
NE_0	0.166 μmol	Amount of residual NE left (NE_0) in presynaptic neurons	[70]
k/b	18.0	Parameter in Nunez's equation	[65]
r	5.8 cm	Average distance from the servers as P300 generators to the scalp	[20, 21]
t_p	100 ms	Duration that NE_{LC} reaches its peak	[19]
NE_{cond}	65 ms	Average to conduction time from the LC to forebrain	[71]

is about 118.6 fmol/μl. Because 1 fmol $= 10^{-15}$ mol (http://pubs.usgs.gov/of/2004/1392/pdf/ofr20041392.pdf, accessed on December 12, 2006) and human brain's volume is about 1400 ml (i.e., $1.4 * 10^6$ μl), therefore, $\mathrm{NE}_0 = 118.6 * 10^{-15} * 1.4 * 10^6 = 166 * 10^{-9}$ mol $=$ 0.166 μmol.

3) k/b: Based on [64, Fig. 4], the difference between the amplitude in control condition and the condition of 10 μm of NE that was injected is $275 - 140 = 135$ μV. Therefore, 1 μm of NE produces about 13.5 μV in the amplitude change of the brain potential

$$\phi = \frac{kS}{4\pi r(b/\mathrm{NE}r)} = (k/b)\frac{S\mathrm{NE}r}{4\pi r}$$

$$13.5 = (k/b)\frac{1 * 1}{4\pi r} => (k/b) \text{ for rabbit is} = 0.154$$

where $r = 0.1$ cm $= 0.001$ m (based on the radius of bulb of a rabbit). For human whose brain is 1400 g which is 1400/12 times that of a rabbit, this ratio changed to $k/b = 0.154 * (1400/12) = 18$.

4) r: Based on measurement data in the figure below (see Fig. 2 in this paper developed based on [19] and [20]), the average distance from the servers as P300 generators (central point of the servers) to the scalp is 5.8 cm.
5) t_p: t_p is defined as the time interval between the arrival of information of stimuli at the LC–NE system $(t = 0)$ and the time point when $\mathrm{NE_{LC}}$ reaches its peak. Its value is set based on [18, Fig. 3] (control condition): the duration of the shadowed area, approximately 100 ms.
6) $\mathrm{NE_{cond}}$: $\mathrm{NE_{cond}}$ is set directly based on the sentence in [70, p. 411]: "LC impulses on reach the frontal cortex is 60–70 ms."

APPENDIX II
THREE CONDITIONS IN RELATING THE DIFFICULTY LEVEL OF TASK 1 AND THE CHANGE OF ϕ_2

Condition 1) $((\partial\phi_2)/(\partial TD_1)) > 0$ (see (24), shown at the previous page).

Solving equations A) and B), we have (25), shown at the previous page. If α and β satisfy (25) [i.e., equations A) and B)] at the same time, i.e., α is lower than the threshold (Γ), an increase of Task 1 difficulty level will increase the value of ϕ_2.

Condition 2) $((\partial\phi_2)/(\partial \mathrm{TD}_1)) < 0$ (see (26), shown at the previous page). If α and β satisfy (26), i.e., α is higher than the threshold (Γ), an increase of Task 1 difficulty level will decrease the value of ϕ_2.

Condition 3) $((\partial\phi_2)/(\partial \mathrm{TD}_1)) = 0$ (see (27), shown at the previous page). Thus, (see (28), shown at the previous page). If α and β satisfy (28), an increase of Task 1 difficulty level will not affect the value of ϕ_2.

ACKNOWLEDGMENT

The authors would like to thank the Associate Editor and several anonymous reviewers for their helpful comments on this paper. They would also like to thank the comments and suggestions from M. Berman in the Department of Psychology and Industrial Operations Engineering, University of Michigan, Ann Arbor, and from C. Drucker and G. Zhao in the Department of Industrial and Systems Engineering, State University of New York, Buffalo.

REFERENCES

[1] Y. Liu, "Queuing network modeling of elementary mental processes," *Psychol. Rev.*, vol. 103, no. 1, pp. 116–136, 1996.
[2] Y. Liu, "Queuing network modeling of human performance of concurrent spatial and verbal tasks," *IEEE Trans. Syst., Man, Cybern. A, Syst., Humans*, vol. 27, no. 2, pp. 195–207, Mar. 1997.
[3] B. Xie and G. Salvendy, "Review and reappraisal of modeling and predicting mental workload in single-and multi-task environments," *Work Stress*, vol. 14, no. 1, pp. 74–99, Jan. 2000.
[4] N. Moray, "Mental workload since 1979," *Int. Rev. Ergonom.*, vol. 2, pp. 123–150, 1988.
[5] C. Wickens, J. Lee, Y. Liu, and S. Gordon-Becker, *Introduction to Human Factors Engineering*. Englewood Cliffs, NJ: Prentice-Hall, 2003.
[6] P. S. Tsang and M. A. Vidulich, *Principles and Practice of Aviation Psychology*. Mahwah, NJ: Lawrence Erlbaum Assoc., 2003.
[7] A. Johnson and R. W. Proctor, *Attention*. London, U.K.: SAGE, 2004.
[8] A. Kramer, "Physiological metrics of mental workload: A review of recent progress," in *Multiple Task Performance*, D. Damos, Ed. London, U.K.: Taylor & Francis, 1991, pp. 279–328.
[9] M. G. H. Coles, G. Gratton, and M. Fabiani, "Event-related brain potentials," in *Principles of Psychophysiology: Physical, Social, and Inferential Elements*, J. T. Cacioppo and L. G. Tassinary, Eds. Cambridge, U.K.: Cambridge Univ. Press, 1990, pp. 413–455.
[10] E. Donchin, "Event-related brain potentials: A tool in the study human information processing," in *Evoked Potentials and Behavior*, H. Begleiter, Ed. New York: Plenum, 1979, pp. 13–75.
[11] E. Donchin, Surprise! . . . Surprise? *Psychophysiology*, vol. 18, pp. 493–513, 1981.
[12] E. Donchin and M. G. H. Coles, "Is the P300 component a manifestation of context updating?" *Behav. Brain Sci.*, vol. 11, pp. 355–372, 1998.
[13] M. D. Rugg and M. G. H. Coles, *Electrophysiology of Mind*. New York: Oxford Univ. Press, 1995.

[14] C. Wickens, A. Kramer, L. Vanasse, and E. Donchin, "Performance of concurrent tasks—A psychophysiological analysis of the reciprocity of information-processing resources," *Science*, vol. 221, no. 4615, pp. 1080–1082, Sep. 1983.

[15] R. Parasuraman, "Event-related brain potentials and human factors research," in *Event-Related Brain Potentials*, J. W. Rohrbaugh, R. Parasuraman, and R. Johnston, Jr., Eds. London, U.K.: Oxford Univ. Press, 1990.

[16] R. C. O'Reilly, "Six principles for biologically based computational models of cortical cognition," *Trends Cognit. Sci.*, vol. 2, no. 11, pp. 455–462, Nov. 1998.

[17] S. Nieuwenhuis, G. Aston-Jones, and J. D. Cohen, "Decision making, the P3, and the locus coeruleus–norepinephrine system," *Psychol. Bull.*, vol. 131, no. 4, pp. 510–532, Jul. 2005.

[18] S. Nieuwenhuis, M. S. Gilzenrat, B. D. Holmes, and J. D. Cohen, "The role of the locus coeruleus in mediating the attentional blink: A neurocomputational theory," *J. Exp. Psychol.-Gen.*, vol. 134, no. 3, pp. 291–307, Aug. 2005.

[19] D. E. Haines, *Fundamental Neuroscience*. New York: Churchill Livingstone, 2002.

[20] M. F. Bear, B. W. Connors, and M. A. Paradiso, *Neuroscience: Exploring the Brain*, 8th ed. Baltimore, MD: Williams & Wilkins, 2001.

[21] C. W. Berridge and B. D. Waterhouse, "The locus coeruleus–noradrenergic system: Modulation of behavioral state and state-dependent cognitive processes," *Brain Res. Rev.*, vol. 42, no. 1, pp. 33–84, Apr. 2003.

[22] C. Wickens, "Applications of event-related potentials to problems in human factors," in *Event-Related Brain Potentials*, J. W. Rohrbaugh, R. Parasuraman, and R. Johnston, Jr., Eds. London, U.K.: Oxford Univ. Press, 1990.

[23] W. H. Levison, "A model for mental workload in tasks requiring continuous information processing," in *Mental Workload: Its Theory and Measurement*, N. Moray, Ed. New York: Plenum, 1979, pp. 189–218.

[24] N. Moray, M. I. Dessouky, B. A. Kijowski, and R. Adapathya, "Strategic behavior, workload, and performance in task scheduling," *Hum. Factors*, vol. 33, no. 6, pp. 607–629, 1991.

[25] W. B. Rouse, *Systems Engineering Models of Human–Machine Interaction*. New York: North Holland, 1980.

[26] S. Baron and K. Corker, "Engineering-based approaches to human performance modeling," in *Applications of Human Performance Models to System Design*, G. R. McMillan, D. Beevis, E. Salas, M. H. Strub, R. Sutton, and L. V. Breda, Eds. New York: Plenum, 1989, pp. 203–218.

[27] G. P. Chubb, K. R. Laughery, and A. B. Pritsker, "Simulating manned systems," in *Handbook of Human Factors & Ergonomics*, G. Salvendy, Ed. New York: Wiley, 1987.

[28] R. M. Harris, F. Glenn, H. P. Iavecchia, and A. Zaklad, "Human operator simulator," in *Trends in Ergonomic: Human Factors III (Part A)*, W. Karwoski, Ed. Amsterdam: North-Holland, 1986.

[29] W. B. Rouse, S. L. Edwards, and J. M. Hammer, "Modeling the dynamics of mental workload and human performance in complex systems," *IEEE Trans. Syst., Man, Cybern.*, vol. 23, no. 6, pp. 1662–1671, Nov./Dec. 1993.

[30] S. Card, T. P. Moran, and A. Newell, *The Psychology of Human–Computer Interaction*. Hinsdale, NJ: Lawrence Erlbaum, 1983.

[31] D. L. Parks and G. P. Boucek, Jr., *Applications of Human Performance Models to System Design*, G. R. McMillan, D. Beevis, E. Salas, M. H. Strub, R. Sutton, and L. V. Breda, Eds. New York: Plenum, 1989, pp. 203–218.

[32] D. B. Hamilton and C. R. Bierbaum, "Task analysis/workload (TAWL): A methodology for predicting operator workload," presented at the Proc. 34th Annual Meeting Human Factors Society, Santa Monica, CA, 1990.

[33] R. A. North and V. A. Riley, "W/INDEX: A predictive model of operator workload," in *Applications of Human Performance Models to System Design*, G. R. McMillan, D. Beevis, E. Salas, M. H. Strub, R. Sutton, and L. V. Breda, Eds. New York: Plenum, 1989, pp. 203–218.

[34] S. X. Bi and G. Salvendy, "A proposed methodology for the prediction of mental workload, based on engineering system parameters," *Work Stress*, vol. 8, no. 4, pp. 355–371, 1994.

[35] O. David, L. Harrison, and K. J. Friston, "Modeling event-related responses in the brain," *Neuroimage*, vol. 25, pp. 756–770, 2005.

[36] O. David and K. J. Friston, "A neural mass model for MEG/EEG: Coupling and neuronal dynamics," *Neuroimage*, vol. 20, pp. 1743–1755, 2003.

[37] B. H. Jansen and V. G. Rit, "Electroencephalogram and visual-evoked potential generation in a mathematical model of coupled cortical columns," *Biol. Cybern.*, vol. 73, no. 4, pp. 357–366, Sep. 1995.

[38] G. Gratton, M. G. H. Coles, E. J. Sirevaag, C. W. Eriksen, and E. Donchin, "Pre- and post-stimulus activation of response channels: A psychophysiological analysis," *J. Exp. Psychol.: Hum. Percept. Perform.*, vol. 14, no. 3, pp. 331–344, Aug. 1988.

[39] M. Usher and E. J. Davelaar, "Neuromodulation of decision and response selection," *Neural Netw.*, vol. 15, no. 4, pp. 635–645, Jun. 2002.

[40] G. Olsen and J. R. Olsen, "The growth of cognitive modeling in human–computer interaction since GOMS," *Hum.-Comput. Interact.*, vol. 5, no. 2/3, pp. 221–265, Jun. 1990.

[41] Y. Liu, "Queueing network modeling of mental architecture, response time, and response accuracy: Reflected multi-dimensional diffusions," presented at the Annu. Meeting of Math. Psychol. Soc., Memphis, TN, 2005.

[42] B. Faw, "Pre-frontal executive committee for perception, working memory, attention, long-term memory, motor control, and thinking: A tutorial review," *Conscious. Cogn.*, vol. 12, no. 1, pp. 83–139, Mar. 2003.

[43] P. E. Roland, *Brain Activation*. New York: Wiley-Liss, 1993.

[44] E. E. Smith and J. Jonides, "Neuroimaging analyses of human working memory," *Proc. Nat. Acad. Sci. U.S.A.*, vol. 95, no. 20, pp. 12 061–12 068, Sep. 1998.

[45] F. Rieke, D. Warland, R. de Ruyter van Steveninck, and W. Bialek, *Spikes: Exploring the Neural Code (Computational Neuroscience)*. Cambridge, MA: MIT Press, 1997.

[46] J. Taylor, B. Horwitzc, N. J. Shaha, W. A. Fellenzb, H.-W. Mueller-Gaertnera, and J. B. Krausee, "Decomposing memory: Functional assignments and brain traffic in paired word associate learning," *Neural Netw.*, vol. 13, no. 8, pp. 923–940, Nov. 2000.

[47] R. Feyen, "Modeling human performance using the queuing network–model human processor (QN–MHP)," M.S. thesis, Dept. Ind. Operations Eng., Univ. Michigan, Ann Arbor, MI, 2002.

[48] S. R. Simon, M. Meunier, L. Piettre, A. M. Berardi, C. M. Segebarth, and D. Boussaoud, "Spatial attention and memory versus motor preparation: Premotor cortex involvement as revealed by fMRI," *J. Neurophysiol.*, vol. 88, no. 4, pp. 2047–2057, Oct. 2002.

[49] H. Mustovic, K. Scheffler, F. Di Salle, F. Esposito, J. G. Neuhoff, J. Hennig, and E. Seifritz, "Temporal integration of sequential auditory events: Silent period in sound pattern activates human planum temporale," *Neuroimage*, vol. 20, no. 1, pp. 429–434, Sep. 2003.

[50] E. T. Rolls, "Memory systems in the brain," *Annu. Rev. Psychol.*, vol. 51, pp. 599–630, 2000.

[51] P. C. Fletcher and R. N. A. Henson, "Frontal lobes and human memory—Insights from functional neuroimaging," *Brain*, vol. 124, no. 5, pp. 849–881, May 2001.

[52] D. S. Manoach, G. Schlaug, B. Siewert, D. G. Darby, B. M. Bly, A. Benfield, R. R. Edelman, and S. Warach, "Prefrontal cortex fMRI signal changes are correlated with working memory load," *Neuroreport*, vol. 8, no. 2, pp. 545–549, Jan. 1997.

[53] K. Kansaku, T. Hanakawa, T. Wu, and M. Hallett, "A shared neural network for simple reaction time," *Neuroimage*, vol. 22, no. 2, pp. 904–911, Jun. 2004.

[54] A. R. Mitz, M. Godschalk, and S. P. Wise, "Learning-dependent neuronal activity in the premotor cortex—Activity during the acquisition of conditional motor associations," *J. Neurosci.*, vol. 11, no. 6, pp. 1855–1872, Jun. 1991.

[55] A. S. Cook and M. H. Woollacott, *Motor Control: Theory and Practical Applications*. Baltimore, MD: Williams & Wilkins, 1995.

[56] P. F. C. Gilbert, "An outline of brain function," *Cognit. Brain Res.*, vol. 12, no. 1, pp. 61–74, Aug. 2001.

[57] A. M. Gordon and J. F. Soechting, "Use of tactile afferent information in sequential finger movements," *Exp. Brain Res.*, vol. 107, no. 2, pp. 281–292, Dec. 1995.

[58] C. Wu and Y. Liu, "Modeling human transcription typing with queuing network–model human processor," presented at the Proc. 48th Annual Meeting Human Factors and Ergonomics Society, New Orleans, LA, 2004.

[59] C. Wu and Y. Liu, "Modeling psychological refractory period (PRP) and practice effect on PRP with queuing networks and reinforcement learning algorithms," presented at the Proc. 6th Int. Conf. on Cognitive Modeling, Pittsburgh, PA, 2004.

[60] J. Lim and Y. Liu, "A queuing network model of menu selection and visual search," presented at the Proc. 48th Annu. Conf. Human Factors and Ergonom. Soc., New Orleans, LA, 2004.

[61] Y. Liu, R. Feyen, and O. Tsimhoni, "Queueing network–model human processor (QN–MHP): A computational architecture for multitask performance," *ACM Trans. Hum. Comput. Interact.*, vol. 13, no. 1, pp. 37–70, Mar. 2006.

[62] C. Wu and Y. Liu, "Modeling behavioral and brain imaging phenomena in transcription typing with queuing networks and reinforcement learning algorithms," presented at the Proc. 6th Int. Conf. Cognitive Modeling, Pittsburgh, PA, 2004.

[63] P. L. Nunez, *Electric Fields of the Brain*. New York: Oxford Univ. Press, 1981.

[64] C. M. Gray, W. J. Freeman, and J. E. Skinner, "Chemical dependencies of learning in the rabbit olfactory bulb: Acquisition of the transient spatial pattern change depends on norepinephrine," *Behav. Neurosci.*, vol. 100, no. 4, pp. 585–596, Aug. 1986.
[65] A. Kramer, C. Wickens, and E. Donchin, "Analysis of the processing requirements of a complex perceptual-motor task," *Hum. Factors*, vol. 25, no. 6, pp. 597–621, Dec. 1983.
[66] W. Piechulla, C. Mayser, H. Gehrke, and W. Konig, "Reducing drivers' mental workload by means of an adaptive man–machine interface," *Transp. Res. F, Traffic Psychol. Behav.*, vol. 6, no. 4, pp. 233–248, Dec. 2003.
[67] J. F. R. Paton, W. R. Foster, and J. S. Schwaber, "Characteristic firing behavior of cell-types in the cardiorespiratory region of the nucleus tractus solitarii of the rat," *Brain Res.*, vol. 604, no. 1/2, pp. 112–125, Feb. 1993.
[68] N. H. Neff, P. F. Spano, A. Groppetti, C. T. Wang, and E. Costa, "A simple procedure for calculating the synthesis rate of norepinephrine, dopamine and serotonin in rat brain," *J. Pharmacol. Exp. Ther.*, vol. 176, no. 3, pp. 701–709, Mar. 1971.
[69] B. M. G. Nellgard, Y. Miura, G. B. Mackensen, R. D. Pearlstein, and D. S. Warner, "Effect of intracerebral norepinephrine depletion on outcome from severe forebrain ischemia in the rat," *Brain Res.*, vol. 847, no. 2, pp. 262–269, Nov. 1999.
[70] G. Aston-Jones and J. D. Cohen, "An integrative theory of locus coeruleus–norepinephrine function: Adaptive gain and optimal performance," *Annu. Rev. Neurosci.*, vol. 28, pp. 403–450, 2005.
[71] R. Parasuraman, "Neuroergonomics: Research and practice," *Theor. Issues Ergonom. Sci.*, vol. 4, no. 1/2, pp. 5–20, Jan. 2003.
[72] E. A. Byne and R. Parasuraman, "Psychophysiology and adaptive automation," *Biol. Psychol.*, vol. 42, pp. 249–268, 1996.
[73] W. J. Burke, S. W. Li, K. N. Gillespie, H. D. Chung, K. Jagadeesan, and J. H. Joist, "Platelet synthesis of DOPEGAL, the free radical generating metabolite of norepinephrine: Potential target for protective therapy in arteriosclerosis," *Lett. Drug Des. Discov.*, vol. 3, no. 7, pp. 481–487, Sep. 2006.
[74] S. Grid, P. Statements, A. S. A. Website, and P. Version, "Chronic cocaine and amphetamine treatment is associated with changes in rat spinal norepinephrine transporters," *Anesthesiology*, vol. 96, p. A794, 2002.
[75] J. M. Lindquist and S. Rehnmark, "Ambient temperature regulation of apoptosis in brown adipose tissue," *J. Biol. Chem.*, vol. 273, no. 46, pp. 30 147–30 156, Nov. 1998.
[76] K. Masur, B. Niggemann, K. S. Zanker, and F. Entschladen, "Norepinephrine-induced migration of SW 480 colon carcinoma cells is inhibited by beta blockers," *Cancer Res.*, vol. 61, no. 7, pp. 2866–2869, Apr. 2001.
[77] E. Mpofu and L. M. Conyers, "Neurochemistry in the comorbidity of conduct disorder with other disorders of childhood and adolescence: Implications for counselling," *Counseling Psychol. Q.*, vol. 16, no. 1, pp. 37–41, Mar. 2003.
[78] J. A. Nadel and P. J. Barnes, "Autonomic regulation of the airways," *Annu. Rev. Med.*, vol. 35, pp. 451–467, 1984.
[79] K. M. Pirke, "Central and peripheral noradrenalin regulation in eating disorders," *Psychiatry Res.*, vol. 62, no. 1, pp. 43–49, Apr. 1996.
[80] J. D. Sanders, H. K. Happe, and L. C. Murrin, "A transient expression of functional alpha2-adrenergic receptors in white matter of the developing brain," *Synapse*, vol. 57, no. 4, pp. 213–222, Sep. 2005.
[81] M. L. Voorhess, "Low plasma norepinephrine responses to acute hypoglycemia in children with isolated growth hormone deficiency," *J. Clin. Endocrinol. Metabol.*, vol. 59, pp. 790–793, 1984.
[82] F. Xu, R. R. Gainetdinov, W. C. Wetsel, S. R. Jones, L. M. Bohn, G. W. Miller, Y. M. Wang, and M. G. Caron, "Mice lacking the norepinephrine transporter are supersensitive to psychostimulants," *Nat. Neurosci.*, vol. 3, no. 5, pp. 465–471, May 2000.
[83] C. Wu and Y. Liu, "Queuing network modeling of driver workload and performance," in *Proc. 50th Annu. Conf. Human Factors Ergonom. Soc.*, San Francisco, CA, 2006, pp. 2368–2372.
[84] C. Wu and Y. Liu, "Queuing network modeling of age differences in driver mental workload and performance," in *Proc. 50th Annu. Conf. Human Factors Ergonom. Soc.*, San Francisco, CA, 2006, pp. 190–194.
[85] K. Abe, T. Sawada, M. Horiuchi, and K. Yoshimura, "Effects of S-8510, a benzodiazepine receptor partial inverse agonist, on event-related potentials (P300) in monkeys," *Psychopharmacology*, vol. 141, pp. 71–76, Jan. 1999.
[86] E. J. Hammond, K. J. Meador, R. Aung-Din, and B. J. Wilder, "Role of the cholinergic system in the generation of human cognitive evoked potentials," *Neurology*, vol. 37, pp. 346–350, 1987.
[87] A. F. Kramer, L. Trejo, and D. Humphrey, "Assessment of mental workload with task-irrelevant auditory probes," *Biol. Psychol.*, vol. 40, no. 1/2, pp. 83–100, May 1995.
[88] D. A. Morilak, G. Barrera, D. J. Echevarria, A. S. Garcia, A. Hernandez, S. Ma, and C. O. Petre, "Role of brain norepinephrine in the behavioral response to stress," *Prog. Neuro-Psychopharmacol. Biol. Psychiatry*, vol. 29, no. 8, pp. 1214–1224, Dec. 2005.
[89] G. K. Aghajanian and M. A. Rogawski, "The physiological role of alpha-adrenoceptors in the CNS: New concepts from single-cell studies," *Trends Pharmacol. Sci.*, vol. 4, pp. 315–317, 1983.
[90] M. Jiang, E. R. Griff, M. Ennis, L. A. Zimmer, and M. T. Shipley, "Activation of locus coeruleus enhances the responses of olfactory bulb mitral cells to weak olfactory nerve input," *J. Neurosci.*, vol. 16, no. 19, pp. 6319–6329, Oct. 1996.
[91] B. D. Waterhouse, S. A. Azizi, R. A. Burne, and D. J. Woodward, "Modulation of rat cortical area 17 neuronal responses to moving visual stimuli during norepinephrine and serotonin microiontophoresis," *Brain Res.*, vol. 514, no. 2, pp. 276–292, Apr. 1990.
[92] D. J. Woodward, H. C. Moises, B. D. Waterhouse, H. H. Yeh, and J. E. Cheun, "The cerebellar norepinephrine system: Inhibition, modulation, and gating," *Prog. Brain Res.*, vol. 88, pp. 331–341, 1991.
[93] D. J. Woodward, H. C. Moises, B. D. Waterhouse, H. H. Yeh, and J. E. Cheun, "Modulatory actions of norepinephrine on neural circuits," *Adv. Exp. Med. Biol*, vol. 287, pp. 193–208, 1991.
[94] C. Wu and Y. Liu, "Queuing network modeling of driver workload and performance," *IEEE Trans. Intell. Transp. Syst.*, vol. 8, no. 3, pp. 528–537, Sep. 2007.
[95] C. Wu and Y. Liu, "A new software tool for modeling human performance and mental workload," *Q. Hum. Factors Appl.: Ergonom. Des.*, vol. 15, no. 2, pp. 8–14, 2007.
[96] C. Wu and Y. Liu, "Queuing network modeling of transcription typing," *ACM Trans. Comput.-Hum. Interact.*, vol. 15, no. 1, May 2008.

Changxu Wu received the B.S. degree in psychology, with a focus on engineering and mathematical psychology, from Zhejiang University, Hangzhou, China, in 1999, the M.S. degree in engineering psychology and human–computer interaction from the Chinese Academy of Sciences, Beijing, in 2002, and the M.S. and Ph.D. degrees in industrial and operational engineering from the University of Michigan, Ann Arbor, in 2004 and 2007, respectively.

He has been an Assistant Professor with the Department of Industrial and Systems Engineering, State University of New York, Buffalo, since August 2007. He has published papers in the IEEE TRANSACTIONS ON INTELLIGENT TRANSPORTATION SYSTEMS, the *International Journal of Human–Computer Studies*, *Acta Psychologica Sinica*, *Ergonomics in Design*, as well as several other journals. The main theme of his current research is the development of computational models of human performance and mental workload, addressing both fundamental and neurological issues of perceptual–motor behavior and human cognition with their applications in designing intelligent transportation systems.

Dr. Wu received the Outstanding Student Instructor Award from the American Society for Engineering Education at the University of Michigan in 2006. He is a member of the Human Factors and Ergonomics Society, Society of Automobile Engineers, and Cognitive Science Society. He served IEEE and other academic organizations as a Reviewer of the IEEE TRANSACTIONS ON SYSTEMS, MAN, AND CYBERNETICS, the IEEE TRANSACTIONS ON INTELLIGENT TRANSPORTATION SYSTEMS, and *Applied Ergonomics*. He was the Chair of the Cognitive Engineering and Decision Making Technique Group's CE14 Session in Human Factor and Ergonomics Annual Meeting 2007.

Yili Liu (S'90–M'91) received the M.S. degree in computer science and the Ph.D. degree in engineering psychology from the University of Illinois, Urbana, in 1990 and 1991, respectively.

He is an Arthur F. Thurnau Professor and an Associate Professor with the Department of Industrial and Operations Engineering, University of Michigan, Ann Arbor. His research and teaching areas include cognitive ergonomics, human factors, computational cognitive modeling, and engineering aesthetics.

Dr. Liu has published refereed journal articles in *Psychological Review*; the IEEE TRANSACTIONS ON SYSTEMS, MAN, AND CYBERNETICS; *Human Factors; Ergonomics*; as well as several other journals. He is a recipient of the University of Michigan Arthur F. Thurnau Professorship Award (selected by the Provost and approved by the Regents of the University of Michigan), the College of Engineering Education Excellence Award; the College of Engineering Society of Women Engineers Professor of the Year Award (twice a recipient); and the Alpha Pi Mu Professor of the Year Award (five times a recipient). He is a coauthor of a human factors textbook entitled *An Introduction to Human Factors Engineering*. He is a member of the Association for Computing Machinery, the Human Factors and Ergonomics Society, the American Psychological Association, and Sigma Xi.

Christine M. Quinn-Walsh received the B.A. degree in physiology and natural sciences from Trinity College, Dublin, Ireland, in 2001, the Postgraduate Diploma in statistics from the University of Dublin, Dublin, in 2002, and the M.S. degree in neuroscience from the University of Michigan, Ann Arbor. She is currently working toward the Ph.D. degree in neuroscience in the Department of Anesthesiology, University of Michigan.

She was awarded a traineeship from the Gerontology Program, University of Michigan (2004–2006), while researching the neural bases of age-related changes in motor control in humans using functional magnetic resonance imaging. In 2006, she was with the Sleep and Memory Laboratory, under the mentorship of Dr. Gina Poe, to research the effects of REM sleep modulation on learning across the lifespan.